CHEMISTRY OF MATERIALS
Article

Chem. Mater. **2010,** *22,* 2001–2009 2001
DOI:10.1021/cm903824e

Self-Assembled Structures of Semiconductor Nanocrystals and Polymers for Photovoltaics. (3) PbSe Nanocrystal−Polymer LBL Multilayers. Optical, Electrochemical, Photoelectrochemical, and Photoconductive Properties

B. Vercelli,[†] G. Zotti,*[,†] A. Berlin,[‡] and M. Natali[§]

[†]*Istituto CNR per l' Energetica e le Interfasi, c.o Stati Uniti 4, 35127 Padova, Italy,* [‡]*Istituto CNR di Scienze e Tecnologie Molecolari, via C. Golgi 19, 20133 Milano, Italy, and* [§]*Istituto CNR di Chimica Inorganica e delle Superfici, c.o Stati Uniti 4, 35127 Padova, Italy*

Received December 21, 2009. Revised Manuscript Received January 22, 2010

Hybrid materials of lead selenide nanocrystals (PbSe-NCs) and organic polymers were produced through a layer-by-layer (LBL) solution-based deposition technique. Polymer series comprises sulfonate-, carboxylate-, and pyridine-based polymers. Nonaqueous dispersions of oleate-capped PbSe-NCs with 2.4 or 2.8 nm diameter were used. Polymers and PbSe-NCs are alternately deposited on ITO-glass surfaces. PbSe-NCs layers in acetonitrile undergo a sharp and irreversible electroxidation process involving two electrons per PbSe unit and an irreversible reduction process due to reduction of a surface lead(II) shell, which involves 20% of the oxidation charge. The multilayer build-up, monitored by UV−vis spectroscopy and cyclic voltammetry, proceeds with a linear increase in the film absorbance and oxidation stripping charge with the number of adsorbed PbSe layers. FTIR analysis has shown that the layering polymers remove the oleate capping ligands completely. The semiconductor properties of these LBL films were evidenced by photoelectrolchemical and (photo)conduction analysis. Photoelectrochemical (oxygen reduction) and photoconductivity responses are stronger in pyridine- than in carboxylate- and sulfonate-based multilayers, suggesting the occurrence of an efficient trapping of the surface lead(II) shell by pyridine moieties.

Introduction

In a previous report, we described multilayered structures from cadmium selenide nanocrystals (CdSe-NCs) and coordinating polymers,[1] with the predictable intent of extending the investigation to their lead analogues. Lead selenide (PbSe) is in fact a semiconductor material with a direct band gap of 0.27 eV, vs 1.7 eV of CdSe. Because of the high atomic number of the Pb^{2+} cation, relativistic effects localize its valence 6s orbital, making this orbital chemically inactive and transforming this s2p2 column IV element into a pseudodivalent p2 atom. Lead thus forms metal monoselenides just like the column II s^2 Cd atoms do.[2]

Like cadmium selenide, lead selenide nanocrystals (PbSe-NCs) embedded into various materials can be used as quantum dots, particularly in nanocrystal solar cells. Bulk PbSe has a high dielectric constant (250) and its small electron and hole effective mass creates an exciton with a relatively large effective Bohr radius (46 nm), eight times larger than that of CdSe.[3] As a consequence size quantization effects are strongly pronounced in PbSe-NCs and the band gap can be tuned from the bulk value of 0.27 to 1.3 eV.[4] For a comparison of PbSe- and CdSe-NCs, the energy levels of 3 nm nanocrystals are illustrated in Figure 1.

We are in fact interested in the application of PbSe-NCs in solar cells. Half of the sun's power lies in the infrared so that the optimal band-gaps for solar cells in both single-junction and tandem architectures lie beyond 850 nm. However, progress in low-cost, large-area, physically flexible solar cells has instead been made with materials possessing absorption onsets in the visible, such as CdSe-NCs.

Recent advances have been achieved in solution-cast infrared photovoltaics through the use of colloidal quantum dots such as PbSe-NCs. Stable solution-processed photovoltaic devices having 3.6% power conversion efficiency in the infrared have been produced.[5] The use of strongly bound bidentate linkers, such as benzenedithiol, ensures device stability over weeks. Diffusion of electrons and holes over hundreds of nanometers through PbSe-NC solids is chiefly responsible for the high external quantum efficiencies obtained in this new class of devices. Also, a Schottky-junction photovoltaic device based on a

*Corresponding author. Tel: (+39)49-8295868. Fax: (+39)49-8295853. E-mail: g.zotti@ieni.cnr.it.

(1) Zotti, G.; Vercelli, B.; Berlin, A.; Chin, P. T. K.; Giovanella, U. *Chem. Mater.* **2009**, *21*, 2258.
(2) An, J. M.; Franceschetti, A.; Dudiy, S. V.; Zunger, A. *Nano Lett.* **2006**, *6*, 2728.
(3) Yu, W. W.; Falkner, J. C.; Shih, B. S.; Colvin, V. L. *Chem. Mater.* **2004**, *16*, 3318.
(4) Steckel, J. S.; Coe-Sullivan, S.; Bulovic, V.; Bawendi, M. *Adv. Mater.* **2003**, *15*, 1862.
(5) Koleilat, G. I.; Levina, L.; Shukla, H.; Myrskog, S. H.; Hinds, S.; Pattantyus-Abraham, A. G.; Sargent, E. H. *ACS Nano* **2008**, *2*, 833.

Published on Web 02/05/2010

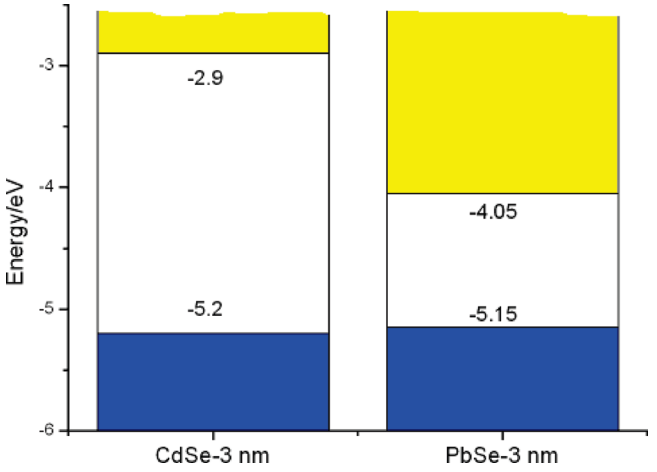

Figure 1. Energy level diagram for 3 nm (left) CdSe-NCs and (right) PbSe-NCs.

thin film of colloidal PbSe-NCs has demonstrated a power conversion efficiency over 2%.[6] The NCs in this device were connected by 1,2-ethanedithiol in a layer-by-layer procedure to produce a conductive NC film.[7] Solar cells based on highly confined nanocrystals of the ternary compound PbS_xSe_{1-x}. have recently been found to be more efficient than pure PbS- or PbSe- based nanocrystal devices.[8]

It is worth noting that the use of PbSe-NCs in photovoltaics is advantageous because of multiple exciton generation (MEG). MEG in semiconductor nanocrystals can produce *n* excitons (*n* is an integer) for each absorbed photon possessing an energy of at least *n* multiples of the band gap energy.

Efficient photodiodes utilizing blends of conjugated polymers with PbSe IR-absorbing quantum dots, have proven elusive at difference with CdSe. Bulk heterojunction devices incorporating blends of PbSe quantum dots and conjugated polymers have produced only 0.1% overall power conversion efficiency.[9,10] PbSe-NCs do in fact sensitize poly(3-hexylthiophene) in a hybrid photovoltaic device into the infrared[9] but the NCs overcoat of 2 nm long oleate ligands poses a barrier for the transport of photocarriers at the surface of the nanoparticle.

To achieve efficient inter-NC coupling in PbSe-NCs, the bulky, native (oleate) capping ligands must be exchanged to allow for smaller inter-NC spacing. CdSe-NC solids may be in fact made more conductive by replacing their original bulky capping ligands with short-chain ligands.[11]

In this report, we describe mono- and multilayers from oleate-capped PbSe-NCs (Chart 1) and coordinating nonpolyconjugated polymers (Chart 2) previously used for CdSe-NCs.[1] To this end, we have used two batches of PbSe-NCs with an average NC diameter of 2.4 and 2.8 nm.

Chart 1

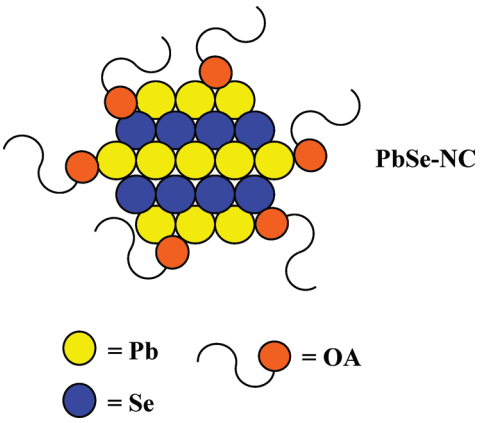

Chart 2

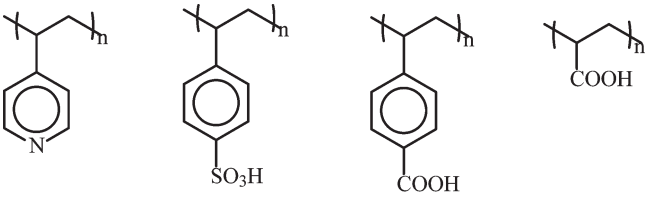

PVPY PSSH PVBH PAAH

The polymers bear coordinating moieties, such as carboxylate, sulfonate, and pyridine, pending from polythene chains (see Chart 2). The carboxylate and sulfonate moieties are linked through a phenylene ring, which makes them structurally comparable with the pyridine moiety and more able to coordinate than when directly linked to the polythene chains, as previously shown for CdSe-NCs.[1] In any case, a polycarboxylate with its carboxylate moieties direct linked to the chain (polyacrylate) has also been considered for comparison.

In the formation of such polymer layers, the PbSe-NCs were expected to behave much the same way of the previously investigated CdSe-NCs[1] because Cd^{2+} and Pb^{2+} are quite similar. Their subsequent stability constants (log K_1; log K_2) for acetate complex formation (1.6; 1.1, and 2.2; 1.4) are in fact very close.

The layers were characterized by UV−vis−NIR spectroscopy, cyclic voltammetry and profilometry and their semiconductor properties were determined by photoelectrochemical and photoconduction analysis.

1. Experimental Section

1.1. Materials. Soluble PbSe-NCs with the surface capped by oleate ligands are produced as described below and detailed in the Supporting Information. In the synthesis, based on reported methods,[12,13] lead(II) oxide and oleic acid are heated at 150 °C in octadecene, and the solution is then cooled to 60 °C, whereby a solution of trioctylphosphine-selenide is subsequently injected. Over the course of minutes, the solution darkens considerably,

(6) Luther, J. M.; Law, M.; Beard, M. C.; Song, Q.; Reese, M. O.; Ellingson, R. J.; Nozik, A. J. *Nano Lett.* **2008**, *8*, 3488.
(7) Luther, J. M.; Law, M.; Song, Q.; Perkins, C. L.; Beard, M. C.; Nozik, A. J. *ACS Nano* **2008**, *2*, 271.
(8) Ma, W.; Luther, J. M.; Zheng, H.; Wu, Y.; Alivisatos, A. P. *Nano Lett.* **2009**, *9*, 1699.
(9) Cui, D.; Xu, J.; Zhu, T.; Paradee, G.; Ashok, S.; Gerhold, M. *Appl. Phys. Lett.* **2006**, *88*, 183111.
(10) Jiang, X. M.; Schaller, R. D.; Lee, S. B.; Pietryga, J. M.; Klimov, V. I.; Zakhidov, A. A. *J. Mater. Res.* **2007**, *22*, 2204.
(11) Yu, D.; Wang, C. J.; Guyot-Sionnest, P. *Science* **2003**, *300*, 1277.
(12) Murray, C. B.; Sun, S.; Gaschler, W.; Doyle, H.; Betley, T. A.; Kagan, C. R. *IBM J. Res. Dev.* **2001**, *45*, 47.
(13) Du, H.; Chen, C.; Krishnan, R.; Krauss, T. D.; Harbold, J. M.; Wise, F. W.; Thomas, M. G.; Silcox, J. *Nano Lett.* **2002**, *2*, 1321.

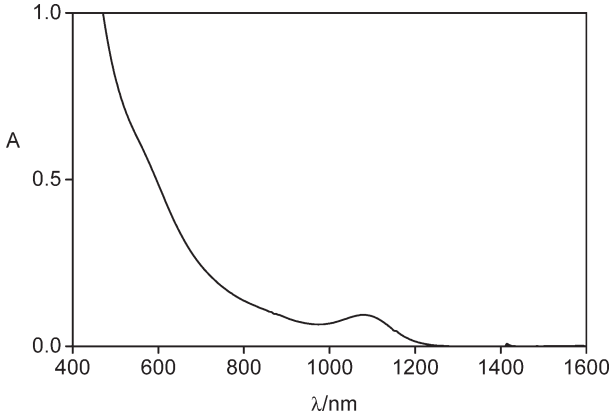

Figure 2. UV−vis−NIR spectrum of 2.8 nm PbSe-NCs in $CHCl_3$.

indicating the formation of the PbSe-NCs. After 30−60 min, the material is isolated by centrifugation and purified by multiple redispersion/precipitation steps in chloroform/methanol.

PbSe-NCs batches with 2.4 or 2.8 nm diameter, determined by TEM, were produced. The electronic spectra of such PbSe-NCs in $CHCl_3$ (a typical spectrum is given in Figure 2) display λ_{max} = 1000 and 1080 nm, respectively.[14] PbSe-NCs dispersions in $CHCl_3$ used for layering were typically 1×10^{-2} M (in PbSe units).

The polymers poly(*p*-styrenesulfonic acid) (PSSH), poly(acrylic acid) (PAAH), poly(vinylbenzoic acid) (PVBH), poly(4-vinylpyridine) (PVPY) and Nafion were purchased from Aldrich. Poly(vinylbenzoic) acid (PVBH) was produced as reported previously.[1] Unless differently stated, they were used in 1×10^{-3} M (in repeat units) concentration in EtOH.

Surface-oleate substitution in PbSe-NC by poly(acrylic acid) (see Results) was performed as follows. A solution of the polymer (1 mg) in THF (5 mL) was added to a solution of PbSe-NCs (8 mg) in $CHCl_3$ (5 mL) and the resulting mixture was stirred overnight. The formed solid precipitate was separated by centrifugation and repeatedly washed with ethanol and dried.

1.2. Substrates and Multilayer Film Formation. Transparent modified surfaces were prepared from glass sheets or indium−tin-oxide (ITO)-glass electrodes (20 Ω sq^{-1} from Merck-Balzers). The ITO-glass electrodes were modified with the different polymers used in this investigation, as reported previously.[1]

The build-up of multilayers (see Scheme 1) was performed on the ITO-glass electrodes according to the methodology introduced by Decher[15] and recently reviewed,[16] i.e., by dipping the electrodes alternatively into the solutions of the two components. Exposing time was 5 min.

1.3. Apparatus and Procedure. *Optical Spectroscopy, Electrochemistry, and Profilometry*. Electronic spectra of layers on ITO-glass electrodes were run on a Jasco V-570 UV−vis−NIR spectrophotometer. Absorbance data are given as measured, i.e., for the sum of the ITO and glass sides, the same level of functionalization being obtained at both sides of the electrode.

Electrochemistry was performed in acetonitrile containing 0.1 M tetrabutylammonium perchlorate (Bu_4NClO_4) as the supporting electrolyte, at room temperature under nitrogen in three electrode cells. The counter electrode was platinum; the reference electrode was a silver/0.1 M silver perchlorate in acetonitrile (0.34 V vs SCE, 4.77 V vs vacuum). The voltammetric apparatus was AMEL, Italy.

Scheme 1

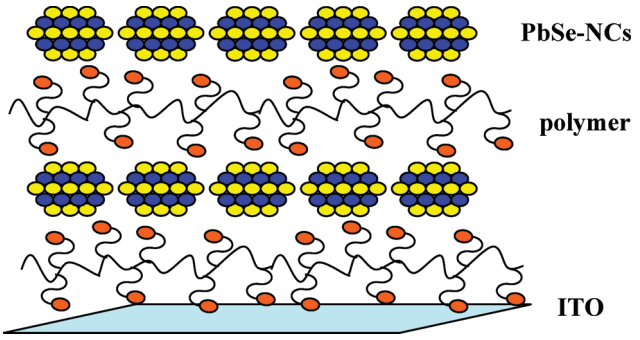

The working electrode for cyclic voltammetry (CV) of cast films was a glassy carbon (GC) minidisc electrode (0.2 cm^2). CV of multilayers was performed on 1 × 4 cm^2 ITO-glass samples with an exposed area of 1 cm^2.

Multilayer thicknesses were determined with an Alphas-step IQ profilometer from KLA Tencor.

IRRAS. FTIR spectra were taken on a Perkin-Elmer 2000 FTIR spectrometer. Infrared Reflection Absorption Spectroscopy (IRRAS) of the layers was performed with a grazing incidence reflection unit (Specac). All spectra were recorded with 2 cm^{-1} resolution at an angle of incidence of 80° relative to the surface normal. Ten cycles were run for each spectrum and weighted subtraction of the background at the end of the series of measurements was applied. No gas purging of the chamber was necessary.

Photoelectrochemistry. Photoelectrochemical experiments were performed in O_2-saturated (unless differently stated) aqueous 0.1 M $NaClO_4$ using a conventional three-electrode cell with a saturated calomel electrode (SCE) as a reference and a platinum counter electrode. All potentials and energies are given with respect to SCE, which is 4.43 eV below the vacuum level. The working electrode was illuminated on the solution side with a water-filtered 100 W halogen lamp, spotted over ca. 10 cm^2. The resulting light power, calibrated with a silicon photodiode, was ca. 100 mW cm^{-2}. Light was chopped with a manually driven shutter.

Conductivity and Photoconductivity. (Photo)conductivity measurements of multilayers were performed with a special Hg electrode contacting the multilayer-covered ITO as described previously.[1] Bias was applied to ITO vs Hg electrode. Illumination (100 mW cm^{-2}) was performed as described above on the back glass side of the ITO/multilayer.

2. Results and Discussion

2.1. Optical and Vibrational Properties of PbSe-NCs. The UV−vis−NIR spectrum of a typical PbSe-NC dispersion in $CHCl_3$ (Figure 2) shows a maximum (first exciton band. $1S_h$-$1S_e$ transition) at 1080 nm corresponding to a diameter of 2.8 nm.[14] The number (n) of PbSe units present in a spherical cluster of Clausthalite (ρ = 8.15 g cm^{-3}) of diameter d (in nm) is given by: $n = 9.0d^3$, so that the value of n calculated in this way for a 2.8 nm cluster is ca. 200. With a crystallographic approach, n (the total number of Pb and Se atoms in a PbSe nanoparticle)

(14) Moreels, I.; Lambert, K.; De Muynck, D.; Vanhaecke, F.; Poelman, D.; Martins, J. C.; Allan, G.; Hens, Z. *Chem. Mater.* **2007**, *19*, 6101.
(15) (a) Decher, G.; Hong, J. *Makromol. Chem. Macromol. Symp.* **1991**, *46*, 321. (b) Decher, G.; Hong, J. *Ber. Bunsenges. Phys. Chem* **1991**, *95*, 1430. (c) Decher, G. *Science* **1997**, *277*, 1232.
(16) Ito, H.; Niimi, Y.; Suzuki, A.; Marumoto, K.; Kuroda, S. *Thin Solid Films* **2008**, *516*, 2743.

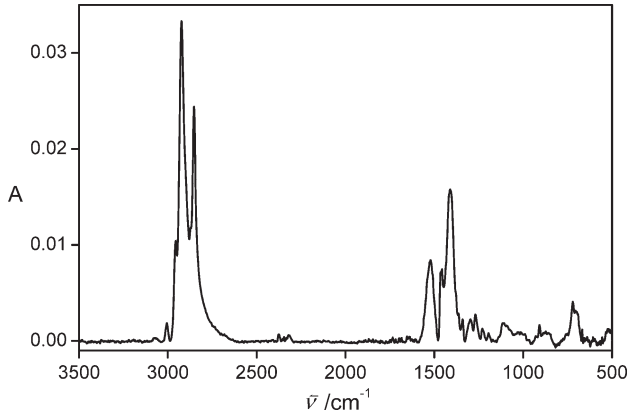

Figure 3. IRRAS spectrum of PbSe-NCs film cast on platinum from $CHCl_3$.

is calculated using the function $n = 4\pi(d/a)^3/3$ based on the bulk crystal structure, where a is the bulk lattice constant, which is 0.612 nm for bulk PbSe crystal.[14] For d = 2.8 nm, n = 400, i.e., 200 PbSe units, in agreement with the calculation above.

Concerning the surface caps, constituted by lead oleate and present as ca. 4 units nm^{-2},[17] the 2.8 nm particles are capped by ca. 100 units. These therefore constitute 42% of the NC mass.

The UV−vis spectrum of the NCs (Figure 2) shows also a strong shoulder at ca. 600 nm, with an intensity 5-fold higher than the exciton band, which we have used to monitor optically the LBL layer growth (see below). The extinction coefficient at 600 nm, referred to PbSe units, is ca. 1000 M^{-1} cm^{-1}.

The FTIR spectrum of the oleate-capped PbSe-NCs film cast on platinum (Figure 3) shows two strong absorption bands at 1522 and 1412 cm^{-1} due to the (COO) asymmetrical and symmetrical stretching modes of the oleate ligand capping the surface of the nanocrystals,[18,19] which indicate the presence of bidentate carboxylate bonding.[20] Strong bands at 2930 and 2850 (stretching), 1470 (scissoring), and 720 (rocking) cm^{-1} are due to the methylene moieties in the alkyl chain of the same oleate ligand. Surface-bound trioctylphosphine (TOP) molecules (surface Se atoms bonded as trialkylphosphine-selenide) are not apparent, in agreement with the negligible TOP content indicated in the literature.[17]

2.2. Growth of PbSe-NC Layers. The formation of layers, routinely investigated by UV−visible spectroscopy monitoring the two-side absorbance of the layer at 600 nm, has provided the following results.

General PbSe Multilayers. Regular layers are obtained with polymers PAAH and PVPY (Figure 4a). PVBH also forms layers but with a peculiar behavior detailed below. Even PSSH, which does not form a priming monolayer on

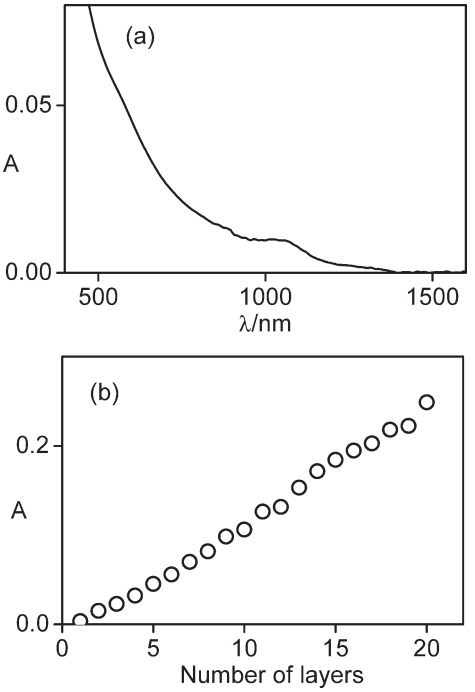

Figure 4. (a) UV−vis−NIR spectrum of a ITO/(PVPY/PbSe)$_5$ multilayer; (b) absorbance at 600 nm of ITO/(PVPY/PbSe)$_n$ multilayers (n = 1−20).

ITO,[1] produced multilayers regularly after an ITO-priming step with PVBH. Thus the hereafter named (PSSH/PbSe)$_n$ multilayers are in fact formed by a first PVBH/PbSe layer and (n − 1) subsequent PSSH/PbSe layers.

A linear increase of PbSe absorbance vs the number of layers (Figure 4b) indicates a stepwise uniform assembly process. The two-side absorbance increase per layer (differential absorbance ΔA), is for all the polymers 12(±2) × 10^{-3} layer^{-1}, corresponding to (2−3) × 10^{-3} layer^{-1} at the first exciton band, i.e., values comparable with those obtained previously with CdSe-NCs.[1] Using the approximate extinction coefficient at 600 nm (ca. 1000 M^{-1} cm^{-1}), the PbSe-NC sublayer content is ca. 6 × 10^{-9} PbSe units mol cm^{-2}, which compared with the polymer coverage of, for example, PVPY (8 × 10^{-10} mol cm^{-2}[21]), indicates a massive insertion of the NCs in the multilayers.

AFM has shown that the multilayers are very uniform. Thickness analysis, performed on 2.4 nm samples (see Table 1), has in general given results compatible with well-packed structures. The (PSSH/PbSe)$_{10}$ and (PVPY/PbSe)$_{10}$ multilayers give a differential thickness d_0 of 1.3 and 1.5 nm layer^{-1}, respectively, compatible with the PbSe crystal size (2.4 nm) in a compact structure. Considering the carboxylic acids, the (PAAH/PbSe)$_{10}$ multilayer is also regularly packed (2 nm layer^{-1}).

PVBH/PbSe Multilayers. The LBL behavior of PVBH is anomalous since the PbSe-NC growth stops after a few layers (see Figure S1a in the Supporting Information). This anomalous behavior is reflected in the thickness of the layers. In fact, the (PVBH/PbSe)$_n$ multilayers display an anomalously high differential thickness of 8 ± 1 nm layer^{-1}, which points to an increase in aggregate formation on the

(17) Moreels, I.; Fritzinger, B.; Martins, J. C.; Hens, Z. *J. Am. Chem. Soc.* **2008**, *130*, 15081.
(18) Shukla, N.; Liu, C.; Jones, P. M.; Weller, D. *J. Magn. Magn. Mater.* **2003**, *266*, 178.
(19) Law, M.; Luther, J. M.; Song, O.; Hughes, B. K.; Perkins, C. L.; Nozik, A. J. *J. Am. Chem. Soc.* **2008**, *130*, 5974.
(20) Young, A. G.; Al-Salim, N.; Green, D. P.; McQuillan, A. J. *Langmuir* **2008**, *24*, 3841.

Table 1. Differential Thickness (d_0) of Multilayers from 2.4 nm PbSe-NCs and Different Polymers; resistance R on $A = 0.023$ cm^2 at 1 V Applied Voltage

multilayer	d_0 (nm layer^{-1})	R (ohm)
$(PVPY/PbSe)_{20}$	1.5	1500
$(PVPY/PbSe)_{10}$	1.5	750
$(PSSH/PbSe)_{10}$	1.3	700
$(PAAH/PbSe)_{10}$	2.0	200
$(PVBH/PbSe)_{10}$[a]	9.0	$>1 \times 10^6$
$(PVBH/PbSe)_{10}$[b]	1.7	250

[a] From 1×10^{-3} M PVBH; [b] From 1×10^{-4} M PVBH;

surface and may account for the progressive blocking of the PbSe-NCs adsorption described above.

Surfactant molecules in solution in fact self-assemble into micellar aggregates at concentrations higher than their critical micelle concentration (CMC).[21] The formation of secondary structures in solutions of polycarboxylic acids including poly(*p*-vinylbenzoic acid) in organic solvents was demonstrated.[22] The secondary structure resulted from interchange H-bonds linking the distant and near monomer units in a degree dependent on the structure of the polymer.[22]

The formation of micelles in our case has been demonstrated and bypassed using a 10-fold lower concentration of PVBH (10^{-4} M) in the same solvent (EtOH) in order to fall below the CMC of the polymer in this medium. Under such conditions the optical growth is linear with a regular slope of 12×10^{-3} layer^{-1}, (see Figure S1b in the Supporting Information) and the differential thickness drops to the regular value of 1.7 nm layer^{-1} (see Table 1). All $(PVBH/PbSe)_n$ multilayers considered hereafter are therefore produced under such micelle-free conditions.

2.3. FTIR Analysis of PbSe-NC Multilayer Growth. IRRAS analysis of multilayer formation on a gold surface has confirmed the regular growth also of the polymeric component and evidenced the progression of ligand substitution in the PbSe-NCs. The polymer used was Nafion, which forms well-defined and stable priming layers on gold[23] as well as on ITO.[24] Moreover, PbSe/Nafion regular multilayers are obtained on Nafion-primed ITO (from 0.1% Nafion) like with the other polymers here investigated, though with a ca. 4 times lower rate. The Nafion progression during multilayer growth was marked by the strong band at 1250 cm^{-1} because of the antisymmetrical stretching mode of the $-CF_2-$ moieties, whereas the contemporary fate of PbSe-NC ligands was followed by the strong C−H stretching band at 2930 cm^{-1} because of the methylene moieties of the oleate ligands.

As far as the polymer progression in concerned, the Nafion-band absorbance increase (ΔA) is proportional with the number of additional Nafion layers (Figure 5).

For the PbSe-NC progression, the monolayer deposited on top of the priming Nafion layer keeps the strong

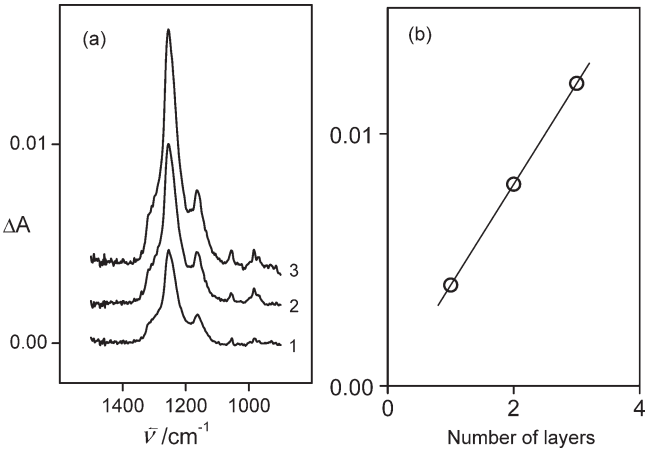

Figure 5. IRRAS spectra and differential absorbance (at 1250 cm^{-1}) of $(PbSe/Nafion)_n$ layers on Nafion-primed gold (to which spectra are referred). Numbers indicate the $(PbSe/Nafion)_n$ layer sequence.

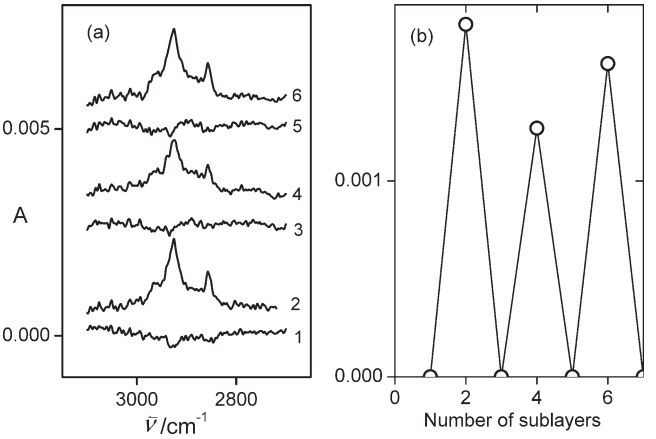

Figure 6. IRRAS spectra and absorbance (at 2930 cm^{-1}) of $(Nafion/PbSe)_n$ layers on gold. Numbers indicate the sublayer (dipping) sequence on the gold surface.

antisymmetrical $-CH_2-$ stretching band at 2930 cm^{-1} but the following Nafion coating causes the complete disappearance of the oleate caps in the surface-bound PbSe-NCs (Figure 6). With subsequent layering the signal reappears with the same intensity at PbSe-NC treatment and disappears with Nafion treatment (Figure 6).

Thus the layers are composed by PbSe-NCs and polymer, the PbSe-NCs being connected by the polymer functional ends and, at least with polysulfonic acids, with the full loss of the originally bound caps (outer PbSe-NC surface excluded). In the layering process, NC and polymer components alternate regularly in the multilayer structure.

The level of surface ligand substitution by the polymers has been checked also for polycarboxylates using poly(acrylic acid) PAAH. However, because the polymers could not in any way be firmly deposited over the IR-reflecting gold surface, we turned to bulk substitution in solution, using a PbSe/PAAH molar ratio of 2, i.e., the same as the oleate-capped NCs (see above). To this end, the polymer was added to PbSe-NCs in solution (see Experimental Section) with the production of a precipitate, insoluble in $CHCl_3$, which confirmed the occurred

(21) Laughlin,R. G. In *The Aqueous Phase Behavior of Surfactants*; Academic Press: San Diego, 1994.
(22) Kuznetsov, N. A.; Roganova, Z. A.; Smolyanskii, A. L. *Vysokomol. Soedin., Ser. A* **1978**, *20*, 791.
(23) Vercelli, B.; Zotti, G.; Berlin, A.; Grimoldi, S. *Chem. Mater.* **2006**, *18*, 3754.
(24) Zotti, G.; Vercelli, B.; Berlin, A. *Chem. Mater.* **2008**, *20*, 6509.

cross-linking of the NCs. The FTIR spectrum of the product as KBr pellet keeps showing the methylene asym stretching band at 2930 cm^{-1}, but this is strongly decreased (10−15 times) compared to the band at ca. 1550 cm^{-1} because of the COO^- asym stretching. Considering that the replaced oleate has 14 methylene moieties versus only 1 in the entering polyacrylate unit, oleate substitution may be assumed to have occurred completely also in this case. The ability of the carboxylate polymer to fully substitute the carboxylate monomeric (oleate) caps is due to entropy factors, namely to the availability of more heads on the same (polymer) molecule for coordination to the PbSe crystal surface.

2.4. Electrochemistry of PbSe-NCs. Electrochemistry of PbSe-NCs has been investigated for the first time very recently.[25] Oleate-capped PbSe quantum dots were cross-linked with 1,7-diaminoheptane and investigated as thin films in anhydrous acetonitrile. Controlled-potential FTIR spectroscopy has shown that both electrons and holes are reversibly injected from an electrode into the quantum confined states. Yet no significant CV signal was detected, probably because of the low amount of applied charge.

As a medium for our electrochemical analysis of cast or multilayer films (from 2.8 nm PbSe-NC samples) we have used acetonitrile +0.1 M Bu_4NClO_4 at room temperature without special techniques to make the medium water-free.

If we consider that the energy levels of 3 nm PbSe (energy gap of 1.1 eV[14]) are at 4.05 and 5.15 eV, (see Figure 1), we should expect oxidation at 0.4 V and reduction at −0.7 V vs Ag/Ag^+. In comparison with CdSe, the oxidation of PbSe-NCs should be displayed at comparable potential values, whereas reduction should be easier by ca. 1 V.

PbSe-NC Cast Films. Films cast from $CHCl_3$ on GC electrodes (Figure 7) show a strong irreversible oxidation process (B) at E_p = ca. 1.2 V, preceded by a lower irreversible process (A) at E_p = ca. 0.35 V, as for the CdSe case previously investigated[1] and attributed to the two-electron oxidation of bulk and surface PbSe units, respectively. In such processes, the selenide anion undergoes oxidation to selenium(0) forms, as found for the photochemical oxidation of indium selenide.[26] Because a $Pb(ClO_4)_2$ solution in acetonitrile does not show any significant anodic response up to 2.5 V at the GC electrode, the remote possibility that the anodic dissolution of the PbSe-NCs includes a two-electron oxidation of Pb(II) to a Pb(IV) form is therefore ruled out.

Differently from the CdSe case, CV scan down to −2.0 V does detect a reduction peak (C) (at E_p = ca. −1.8 V), irreversible and of intensity lower than that of oxidation peak (B), which is attributed to the two-electron reduction of some Pb^{2+} in the crystals.

The charge for oxidation (A + B) is ca. 5 times that for reduction (C), and since such charges correspond both to two-electron processes, the reduction appears to involve a

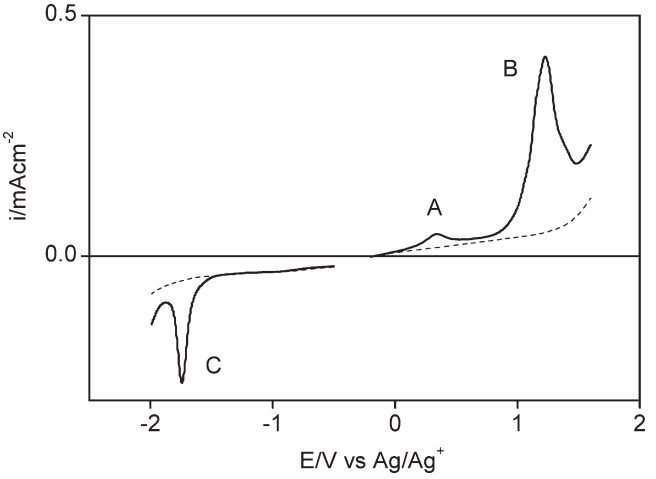

Figure 7. Single-sweep voltammograms of (A, B) oxidation and (C) reduction of PbSe-NCs layer on GC electrode in acetonitrile + 0.1 M Bu_4NClO_4. Scan rate: 0.02 V s^{-1}.

Pb^{2+} content ca. 20% of that of PbSe. Moreover the reduction charge is independent from the scan rate, (from 0.02 to 0.1 V s^{-1}), which rules out transport limitations to the process, such as a slow and progressive reduction of the bulk PbSe units. Instead, the result points to the presence of an oxidized lead shell on the PbSe-NC surface, normally encountered in such NCs.[14]

PbSe-NC Layers. Similarly with the cast films, CV analysis of the ITO/$(PAAH/PbSe)_n$ layers shows two irreversible oxidative processes at E_p = ca. 0.5 and 1.8 V, as a whole due to the two-electron oxidation of selenide in the PbSe units, in which a net total charge of 0.8 mC cm^{-2} per layer is involved (at 2.2 V switching potential). Such anodic stripping processes involve the complete dissolution of the deposits. Similar results are obtained from PSSH-layers.

The anodic stripping charge, which is comparable with that previously measured for CdSe-NCs of the same size,[1] is somewhat lower than that (1.2 mC cm^{-2}) calculated from the optical values but these are affected by a conspicuous degree of uncertainty on the extinction coefficient.

PVBH is distinguished also in this case. CV oxidation analysis of the ITO/$(PVBH/PbSe)_n$ layers (Figure 8a) has shown the two irreversible oxidative processes at E_p = ca. 0.4 and 1.6 V, in which a net total charge of once more 0.8 mC cm^{-2} per layer is involved, but the charge is located essentially in the first anodic process. This may be attributed to a strong stabilization of the Pb^{2+} ions, made free in the oxidation, from coordination of the cross-linking benzoate moieties in the polymer layers, available in a high amount and sterically more able to coordination.

Also, the cathodic CV of these PVBH/PbSe multilayers is anomalous. CV down to −2.0 V shows two reduction processes (at E_p = ca. −1.45 and −1.7 V, Figure 8b) instead of the one (around −1.7/−1.8 V) in the cast layers. The overall reduction charge is once more ca. 20% of the oxidation charge, independently of the scan rate, which supports the results from cast films of PbSe-NCs.

The reason for the more favorable reduction process, which we have assigned to the Pb^{2+} surface species, may

(25) Wehrenberg, B. L.; Guyot-Sionnest, P. *J. Am. Chem. Soc.* **2003**, *125*, 7806.
(26) Dimitrijevic, N. M.; Kamat, P. V. *Langmuir* **1987**, *3*, 1004.

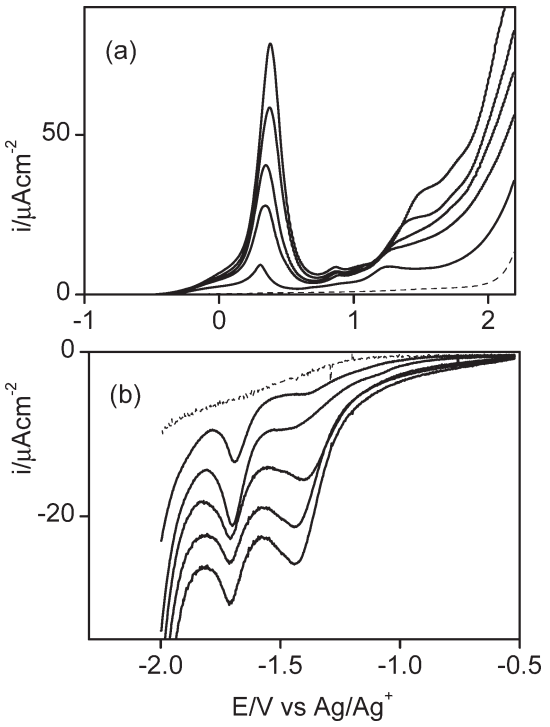

Figure 8. Single-sweep voltammograms of (a) oxidation and (b) reduction of ITO/(PVBH/PbSe)$_n$ multilayers (n = 1−5) in acetonitrile + 0.1 M Bu_4NClO_4. Scan rate: 0.02 V s^{-1}.

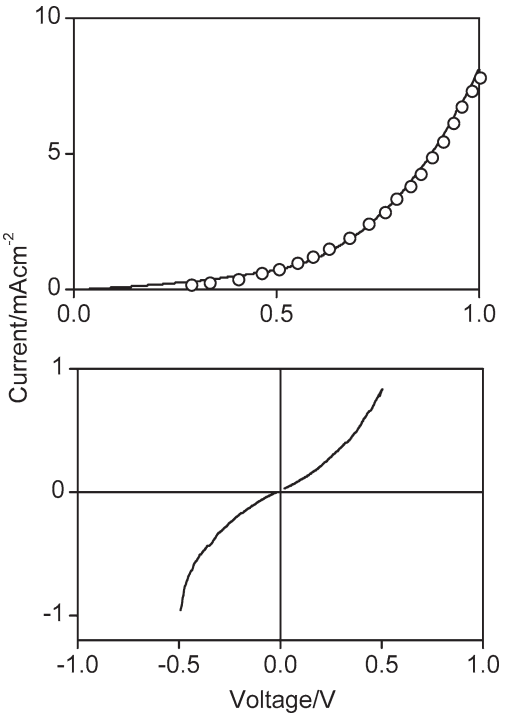

Figure 9. $I-V$ plot of ITO/(PVPY/PbSe)$_{20}$ multilayer (2.4 nm). Dots: fitting of Simmoms equation.

be found in the lower nucleophilic power of the coordinating aromatic (benzoate) compared with aliphatic anions in the oleate-capped photoelectrochemical. This suggestion has been confirmed by CV of a Pb(II) polyvinylbenzoate film produced as detailed in the Supporting Information. The CV response, shown in Figure S2 in the Supporting Information, evidence the reduction of the polymeric salt deposit at $E_p = -1.6$ V, i.e., at a potential close to that of the first reduction process of the PbSe-NC layers. It must be pointed out that the same experiments, performed with PAAH (containing aliphatic carboxylate anions) in place of PVBH, have not given any significant CV response in the same potential range.

2.5. Conductivity. *Dark Conductivity*. The conductivity of multilayers could be measured with the Hg-contact probe. The results from 2.4 nm samples, as resistance measured at 1 V applied voltage, are summarized in Table 1.

In ITO/(PVPY/PbSe)$_n$ multilayers, produced with n = 10 and 20, the resistance was found to be proportional with the number of layers. Anyway the $i-V$ plot is not linear (Figure 9) but fits the Simmons equation for tunneling through a rectangular barrier,[27] which provides a support for nonresonant tunneling as the transport mechanism.

In ITO/(PSSH/PbSe)$_n$ and ITO/(PVBH/PbSe)$_n$ multilayers the $i-V$ plot is the same and approximately linear (ohmic) in both directions though some rectification (factor of ca. 3 at 1 V) is apparent due to the asymmetry of the contacts (Figure 10). In ITO/(PAAH/PbSe)$_n$ multilayers, the $i-V$ plot is regularly ohmic with no rectification and a relatively high conductivity. This is the first distinctive feature of such layers compared with the PVPY layer. The conductivity of these layers is in any case low ($1-4 \times 10^{-7}$ S cm^{-1}).

Charge transport in an array of close-packed semiconductor nanocrystals separated by thin barriers can in fact occur by hopping between quantum-confined orbitals with S and P symmetry. The conductivity of a typical PbSe wirelike assembly is estimated as 7 S cm^{-1}.[28] This value is substantially higher than the corresponding value in polycrystalline PbSe thin films, comprised of microsized grains (5×10^{-2} S cm^{-1})[29] but close to the conductivity in a PbSe two-dimensional quantum well structure (10−20 S cm^{-1}).[30] Therefore, arrays of lead chalcogenide nanocrystals are expected to show in general optimal charge transport properties.[31] Past studies have on the contrary revealed low electronic conductivity because of poor exchange coupling and large concentrations of surface dangling bonds that trap carriers in midgap states.[32,33]

Photoconductivity. Photocurrent transients of ITO/(PVPY/PbSe)$_{20}$ multilayer at 1 V applied voltage and 100 mW cm^{-2} illumination are shown in Figure 11. The strong response (4 mA cm^{-2}) is indicative of a highly

(27) Engelkes, V. B.; Beebe, J. M.; Frisbie, C. D. *J. Am. Chem. Soc.* **2004**, *126*, 14287.

(28) Sashchiuk, A.; Amirav, L.; Bashouti, M.; Krueger, M.; Sivan, U.; Lifshitz, E. *Nano Lett.* **2004**, *4*, 159.

(29) Kumar, S.; Hussain, M.; Sharma, T. P.; Husain, M. *J. Phys. Chem. Solids* **2003**, *645*, 367.

(30) Rogacheve, E. I.; Tavrina, T. V.; Nashchekina, O. N.; Grigorov, S. N.; Nasedkin, K. A.; Dresselhaus, M. S.; Cronin, S. B. *Appl. Phys. Lett.* **2002**, *80*, 2690.

(31) Talapin, D. V.; Murray, C. B. *Science* **2005**, *310*, 86.

(32) Jarosz, M. V.; Porter, V. J.; Fisher, B. R.; Kastner, M. A.; Bawendi, M. G. *Phys. Rev. B* **2004**, *70*, 195327.

(33) (a) Ginger, D. S.; Greenham, N. C. *J. Appl. Phys.* **2000**, *87*, 1361. (b) Morgan, N. Y.; Leatherdale, C. A.; Drndić, M.; Jarosz, M. V.; Kastner, M. A.; Bawendi, M. *Phys. Rev. B* **2002**, *66*, 075339. (c) Vanmaekelbergh, D.; Liljeroth, P. *Chem. Soc. Rev.* **2005**, *34*, 299.

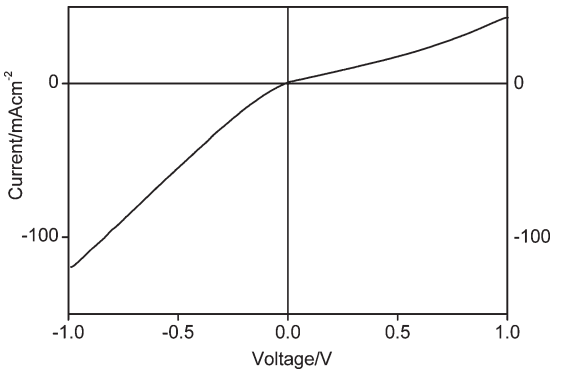

Figure 10. $I-V$ plot of ITO/(PSSH/PbSe)$_{15}$ multilayer (2.4 nm).

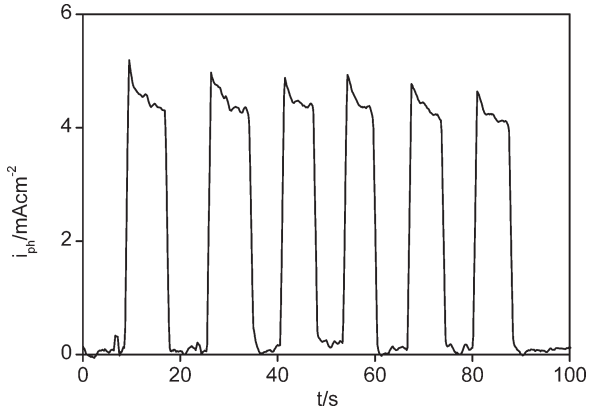

Figure 11. Photocurrent transients of ITO/(PVPY/PbSe)$_{20}$ multilayer at 1 V applied voltage and 100 mW cm^{-2} illumination.

efficient photogeneration of carriers. The response increases with the thickness (in the 10-layer system, it is about half of that in the 20-layer one), thus regularly running the opposite direction of the dark conductivity.

As summarized in Table 2, also in ITO/(PVBH/PbSe)$_{20}$ multilayers, photocurrents are obtained though they are 5 times lower. On the contrary, in the ITO/(PAAH/PbSe)$_{20}$ multilayers, which are the most conductive, the photoconductivity is even lower, below the detection limit of the used method. Similarly, no photocurrent transient was obtained from ITO/(PSSH/PbSe)$_{20}$ multilayer under the same conditions.

2.6. Photoelectrochemistry. Photoelectrochemistry (PEC) is a powerful tool for the investigation of the charge transfer ability of semiconductor (including PbSe-NCs) layers. The photovoltaic properties of our hybrid multilayers have been investigated in a liquid-junction arrangement, i.e., immersed in aqueous electrolyte containing oxygen as a photoelectron acceptor. Under illumination, charge separation is measured as a photocurrent in the external circuit. In more details, light of energy greater than the band gap in the nanoparticle creates an excited state, which can decay via intraparticle recombination of the electron and hole or via transfer of charge to the electrode. If an electron acceptor (or "electron scavenger", oxygen in our case) is present in the solution, the excited electron can be transferred to the solution generating a photocurrent in the external circuit.

Table 2. Limiting Photocurrents i_L (in O_2-saturated 0.1 M $NaClO_4$) and Solid-State Photocurrents i_{ph} (at 1 V applied voltage 1 between ITO-Hg contacts) for 2.4 nm PbSe-NC Multilayers under 100 mW cm^{-2} Illumination

multilayer	i_L (μA cm^{-2})	i_{ph} (mA cm^{-2})
(PVPY/PbSe)$_{20}$	200	
(PVPY/PbSe)$_{10}$	100	
(PSSH/PbSe)$_{10}$	20	
(PAAH/PbSe)$_{10}$	20	
(PVBH/PbSe)$_{10}$[a]	10	
(PVPY/PbSe)$_{20}$		4.0
(PSSH/PbSe)$_{20}$		<0.05
(PAAH/PbSe)$_{20}$		<0.05
(PVBH/PbSe)$_{20}$[a]		0.8

[a] From 1×10^{-4}MPVBH.

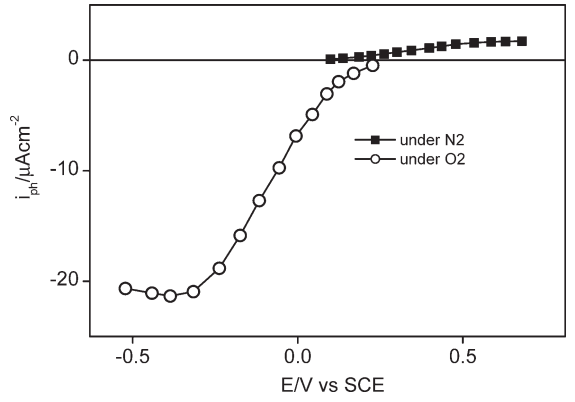

Figure 12. Photocurrent response in linear sweep voltammetry (v = 0.005 V s^{-1}) for ITO/(PSSH/PbSe)$_{10}$ multilayer in (O) O_2- and (■) N_2-saturated 0.1 M $NaClO_4$.

The electrochemical junction presents the advantage of an easy realization but also the risk that semiconductor NCs undergo photoanodic degradation. We have in any case observed that the absorption spectrum of PbSe-NCs before and after PEC analysis is essentially the same, which guarantees that degradation, if any, is in fact minimal.

As a typical example Figure 12 shows the photocurrent−potential plot of an ITO/(PSSH/PbSe)$_{10}$ electrode in O_2-saturated aqueous 0.1 M $NaClO_4$. The electrode was illuminated on the solution side with chopped light from a halogen lamp. Light-induced reduction currents on a low background current were observed between −0.5 and 0.1 V vs SCE, with no mass transfer control. At potentials more positive than 0.1 V, under both oxygen and nitrogen, anodic photocurrent was observed (Figure 12), corresponding to water photoxidation. Such responses are anyway low (typical plateau values of 2 μA cm^{-2} for 10-bilayers, independently from the polymer used) so that PEC investigations were performed in reduction.

For all the investigated multilayers (from 2.4 nm samples) the reduction photocurrent begins to develop at 0.1−0.2 V (onset potential) and reaches plateau values (limiting photocurrent i_L) different from polymer to polymer. The i_L values (reported in Table 2) are proportional to the number of layers. It may be observed that the i_L values are comparable for the polyanions but 5−10 times higher for PVPY. This follows the photoconductivity measured

in the solid state for the PVPY samples, not appreciable in the case of PSSH-samples.

These overall results appear to indicate a sluggish hole-promoted photoconductivity, but a strongly enhanced photoelectron conduction in PbSe-NCs.

2.7. Comparison of Photoconductive Properties of PbSe- and CdSe-NCs. A realistic model for colloidal PbSe-NCs consists of a faceted spherical nanocrystal, with a central Pb or Se atom and composed of a quasi-stoichiometric PbSe core terminated by a Pb surface shell.[14] It is on this oxidized Pb layer that the anions of the oleate surfactant are grabbed and as a consequence the organic capping of colloidal PbSe nanocrystals consists primarily of tightly bound oleate ligands, with only a minor part (0−5% in mole fraction) of the ligand shell composed of TOP.[17] Therefore anionic functionalities of the substituting polymer will coordinate the outer oxidized Pb layer of the PbSe-NC.

The photoconductive properties are dependent on the type of polymer functionalities, the photoconductvitivity increasing in the order $-SO_3^- < -COO^- <$ pyridine. In particular, the sulfonate-based polymer is not photoconductive. This is right the inverse order found in the corresponding CdSe-NC structures.[1] We suggest that this result is attributable to the presence of the lead shell capping the PbSe core, which acts as a site for electron−hole traps or recombination centers. The sulfonate moiety is not nucleophilic enough, whereas carboxylate and even more pyridine are strongly coordinating moieties, able to block such centers and easing therefore transport of photogenerated carriers.

The same core-capping lead shell may be responsible for the absence of a significant photoelectrochemical oxidation of water, which on the contrary is very efficient in the CdSe-NC conterparts.[34]

(34) Zotti, G.; Vercelli, B.; Berlin, A.; Pasini, M.; Nelson, T. L.; McCullough, R. D.; Virgili, T. *Chem. Mater.* **2010**, in press.

Conclusions

PbSe-NC multilayers have been successfully deposited in alternation with sulfonate-, carboxylate-, and pyridine-based polymers.

The layers in organic medium are irreversibly oxidized with two electrons per PbSe unit and reduced with 20% of the oxidation charge at a surface lead(II) shell. This latter is responsible for the photoconductivity response, which is high only for the pyridine-based, possibly trap-blocking, polymer layers.

The produced hybrid structures, formed by organic polymers and semiconductor nanocrystals, easily produced from solution of low-cost materials, offer favorable perspectives for hybrid organic−inorganic solar cells operating in the infrared region of the solar spectrum.

Acknowledgment. The authors thank S. Sitran of the CNR for his technical assistance.

Supporting Information Available: Synthesis of PbSe-NCs; analysis of multilayer growth in different concentations of PVBH; synthesis and CV of Pb(II) polyvinylbenzoate films (PDF). This material is available free of charge via the Internet at http://pubs.acs.org.